METHOD TO PREDICT EXTERNAL STORE CARRIAGE LOADS AT TRANSONIC SPEEDS*

Bruce S. Rosen
Grumman Aircraft Systems Division
Bethpage, New York

SUMMARY

A computational method developed to provide an inviscid transonic analysis for isolated and underwing, pylon-mounted stores is described. Wing, fuselage, pylon, and store body and fin components are modelled simultaneously by computing solutions on a five-level embedded grid arrangement. Flow field accuracy in the vicinity of the store is enhanced by the use of cylindrical grids which conform to the actual store body shape. A completely automated grid generation procedure facilitates applications. A finite difference scheme developed specifically for modified transonic small disturbance flow equations enhances the method's numerical stability and accuracy. Treatment of lower aspect ratio, more highly swept and tapered wings is therefore possible. A limited supersonic freestream capability is also provided. For the test cases considered, computed surface pressures and load distributions reveal strong store/airframe interactions. Predicted results are supported by correlations with experimental data. It is concluded that predictions would be improved by simple 2-D or axisymmetric modelling of viscous effects and flow separation.

INTRODUCTION

Prediction of external store carriage characteristics at transonic speeds requires computations for rather complex geometries. Wing, fuselage, pylon, and store body and fin components each need to be modelled. While methods to obtain full potential, Euler, and Navier Stokes solutions for simpler geometries are maturing at a rapid pace, transonic small disturbance (TSD) formulations are still a practical alternative for treatment of these more complex configurations.

The NASA/Grumman Transonic Wing-Body Code (refs. 1,2,3) represents the state of the art for reliable TSD analysis of complex aircraft. An attempt to extend similar wing/fuselage methodology to treat wing/fuselage/pylon/store geometries (refs. 4,5) attributed poor isolated body normal force correlations to the TSD formulation. Since approaches emphasizing the use of more sophisticated flow equations (refs. 6,7,8) are difficult to implement and require further development for practical three-dimensional applications, a more accurate TSD formulation was developed for treatment of store body shapes (ref. 9). This approach was then employed for more accurate treatment of finned stores and store carriage configurations.

---

*This work was supported by NASA Contract NAS1-18105.

The Transonic Store Carriage Loads Prediction (TSCLP) Code which was developed combines refined TSD approaches (refs. 1,2,3,9) for treatment of isolated and underwing, pylon-mounted stores. TSCLP Code prediction accuracy for isolated stores with multiple fore and aft fins was documented in reference 10. For the single pylon-mounted store test case considered, good correlation was also shown in reference 10 between computed and experimental store body surface pressures and load distributions. In this paper, after presenting an overview of the computational method, TSCLP Code prediction capability for store carriage configurations is evaluated in more detail.

SYMBOLS

b	wing span
C_p	pressure coefficient
c_y	store body cross-section side force coefficient
c_z	store body cross-section normal force coefficient
L	fuselage or store body length
M_∞	freestream Mach number
RMAX	store body maximum radius
T,U,V	coefficients of governing flow equation
x,r,θ	cylindrical coordinates
x,y,z	Cartesian coordinates
α	angle of attack
γ	specific heat ratio
η	wing spanwise coordinate, 2y/b
ϕ	perturbation potential

COMPUTATIONAL METHOD

Treatment of wing/fuselage/pylon geometry is similar to that found in the basic wing-body code (refs. 1,2). Modelling capability for isolated and underwing, pylon-mounted stores is limited to axisymmetric store bodies with multiple fore and aft fins. Store flow field accuracy is enhanced by the use of cylindrical grids which conform to the actual store body shape. Store fins are then treated using a small disturbance, planar representation analogous to that used for wings and pylons. No provision is made in the computations for modelling of viscous effects and/or flow separation.

A completely automated grid generation procedure facilitates applications. Required inputs consist of configuration geometry, freestream flow conditions, and number of solution iteration cycles. Geometry input verification for a Douglas wing/pylon/store test configuration is shown in figure 1. Grid set up for this geometry is shown in figure 2.

Modified TSD flow equations are employed. These permit calculation of flow nonlinearities, including shocks, and at the same time provide the flexibility required for treatment of complex geometries. In Cartesian grids the flow equation is given by

$$T\,\phi_{xx} + U\,\phi_{xy} + V\,\phi_{yy} + \phi_{zz} = 0$$

where subscripts denote partial differentiation, and

$$T = 1 - M_\infty^2 - (\gamma+1)\,M_\infty^2\,\phi_x - ((\gamma+1)/2)\,M_\infty^2\,\phi_x^2$$

$$U = -2\,M_\infty^2\,\phi_y$$

$$V = 1 - (\gamma+1)\,M_\infty^2\,\phi_x$$

In cylindrical grids the flow equation is similarly given by

$$T\,\phi_{xx} + U\,\phi_{xr} + V\,\phi_{rr} + 1/r\,\phi_r + 1/r^2\,\phi_{\theta\theta} = 0$$

where T and V are as above, and

$$U = -2\,M_\infty^2\,(\alpha \sin\theta + \phi_r)$$

The equations are referred to as modified because additional terms are retained relative to the classical TSD flow equation. The $\phi_x^2\,\phi_{xx}$ term is retained to provide a better approximation to the transition between subsonic and supersonic flow. The $\phi_y\phi_{xy}$, $\phi_x\phi_{yy}$ and $\phi_r\phi_{xr}$, $\phi_x\phi_{rr}$ terms are retained to more accurately resolve shock waves which are swept in the x-y (wing) and x-r (fin) planes, respectively.

Finite difference approximations are substituted into the flow equations to arrive at a tridiagonal, successive line over-relaxation scheme. An upwind, rotated difference scheme (ref. 11) provides the proper domain of dependence at supersonic points. A variation of this scheme developed specifically for modified TSD flow equations (ref. 3) determines the rotation from the coefficients T,U,V rather than from local flow angularities. This greatly enhances the method's numerical stability and accuracy. Treatment of lower aspect ratio, more highly swept and tapered wings is therefore possible.

A supersonic freestream capability is also provided. For this, outermost grid boundaries are located a finite distance from the configuration where appropriate inflow, outflow, and radiation-type boundary conditions (ref. 12) are applied. The supersonic freestream capability works well for wing/fuselage combinations, but only limited success was achieved for treatment of stores.

As shown in figure 2, a five-level embedded grid arrangement is employed. Wing and fuselage components are modelled in Cartesian grids, store body and fin components are modelled in cylindrical grids, and the pylon is modelled in both. The grid generation procedure is currently set up to treat wing/store gaps as small as one store diameter, excluding fins, or one-half store radius, including fins, whichever is larger. Communication between embedded grids is accomplished by interpolation of central first derivatives and, where required, upwind second derivatives of the potential in a direction normal to the computational grid boundaries.

As in the basic wing-body code (refs. 1,2), the global coarse grid and wing fine grid systems are used to model the wing and fuselage. A wing/store interaction (WSI) grid is embedded within the global coarse grid in the vicinity of the store. This medium density grid functions as a means of communication between the other Cartesian grids and the cylindrical grids. There are appropriate gaps or holes in the Cartesian grids where the store geometry is not readily modelled. The flow field in this region is computed using a cylindrical C-grid embedded within the WSI grid. A second, finer, cylindrical C-grid is embedded within the first to further improve solution accuracy.

Along with the use of cylindrical C-grids, the more accurate TSD formulation for store body shapes employs exact body surface boundary conditions and isentropic pressure coefficients. Estimates of incremental store body loads due to viscous crossflow effects (ref. 13) are included along with computed inviscid results. These simple estimates are based solely on the store's combined pitch/yaw angle relative to the freestream flow and, as such, are strictly valid for isolated bodies only.

COMPARISONS AND CORRELATIONS

The first case considered is the Douglas wing/pylon/store test configuration introduced in the previous section. Results computed at $M_\infty = 0.75$ and $\alpha = 4°$ for isolated wing and store components are compared in figures 3-5 to those computed for the wing/pylon/store configuration. Overall, the results show the presence of strong store/airframe interactions.

In figure 3, computed wing chordwise surface pressures are compared to experimental data (ref. 14) obtained at a span station somewhere in the vicinity of the pylon. Even for the wing-alone configuration, correlation on the wing upper surface is poor. Airfoil section studies using the more sophisticated 2-D GRUMFOIL method (ref. 15) gave similar predictions, suggesting that test anomalies, rather than flow simulation inaccuracies, are to blame. Nevertheless, the predicted and measured effect of the pylon and store on wing upper surface pressures is a slightly more pronounced leading-edge expansion.

Correlation with data in figure 3 is better on the wing lower surface. The compression in front of and expansion around the pylon leading edge propagates onto the wing lower surface, with measured pressure levels midway between those computed at the inboard and outboard wing/pylon junction. The flow then accelerates along the length of the pylon. It expands even more as it attempts to fill in behind the rather blunt pylon trailing edge, where it then undergoes the usual trailing-edge compression. The large expansion and strong shock predicted at the pylon trailing edge occur in the data to a lesser degree, possibly due to viscous effects and/or flow separation which have not been modelled.

Computed wing spanload distributions are also shown in figure 3. The combined effect of the wing and store is a marked decrease in wing loading which is greatest at the wing/pylon junction itself. The load carried on the pylon appears as a discontinuity in the wing spanload.

Isolated and pylon-mounted store longitudinal pressure distribution predictions are compared in figure 4. The large compressions and expansions associated with the pylon leading and trailing edges can be seen along the store top centerline. Here, the leading-edge expansion terminates in a shock, after which pressure levels are closer to those on the adjacent wing surface. Aft of the pylon, the flow continues to accelerate slightly, until it is overcome by the compression at the wing trailing edge. These effects occur to a lesser degree along the inboard and outboard sides of the store, and even less so along the bottom centerline.

The predicted effects of the airframe on store axial load distributions are shown in figure 5. Most noticeable is a downward load in the area of the wing and pylon leading edge, an upward load due to the expansion in the immediate wing/pylon/store vicinity, and downward loads near the wing and pylon trailing edges. There are also small excursions in side force.

The second case considered is the same Nielsen wing/fuselage/pylon/store test configuration studied in reference 10. Here, results computed at $M_\infty = 0.925$ and $\alpha = 5°$ for the isolated wing/fuselage and store components are compared in figures 6-8 to those computed for the wing/fuselage/pylon and wing/fuselage/pylon/store configurations. As for the Douglas test configuration, the results show the presence of strong store/airframe interactions.

The predicted effects of pylon and store on wing chordwise pressure distributions at the pylon span station are shown in figure 6. The compressions and expansions at the pylon leading and trailing edges propagate onto the wing lower surface. A slight acceleration otherwise occurs along the length of the wing/pylon junction. These effects are more pronounced when the store is present. The compression at the store nose for this case propagates onto the the wing lower surface, accompanied by a slight increase in the size of the wing leading-edge expansion. The effects of the pylon and store on the wing spanload distribution are also shown in the figure. The pylon without a store has a much smaller effect on the wing spanload than does the pylon/store combination.

Computed fuselage bottom centerline pressure distributions are compared to experimental data (ref. 16) in figure 7. For the wing/fuselage configuration, the wing lower surface pressure field propagates only slightly onto the fuselage bottom centerline. With the pylon present, this effect is enhanced. With both pylon and store present, the effect is highly pronounced. These results correlate well with the data.

In reference 10, computed store pressure and axial load distributions for this configuration (as well as for the isolated store) were compared with experimental data (ref. 16). The pylon-mounted store axial load distributions are shown here again, in figure 8. Good correlation is shown for both normal and side force load distributions. The anomaly in predicted side force in the vicinity of the pylon trailing edge is attributed to a small misalignment of predicted inboard and outboard pylon trailing-edge shock locations. Unfortunately, one of the difficulties encountered in predicting store loads at transonic speeds is that relatively large loads result from rather small differences in surface pressures. Modelling of viscous effects and/or flow separation might correct this computational deficiency.

The Nielsen wing/fuselage/pylon/store configuration was tested at supersonic, as well as subsonic, freestream Mach numbers. Although limited success was achieved for supersonic treatment of stores, calculations for this configuration were possible, most likely because the underwing store is in a region of reduced, lower Mach number flow. Results computed at $M_\infty = 1.1$ and $\alpha = 5°$ are shown in figures 9-11.

In figure 9, which shows results for the wing and fuselage, an unexplained variation in wing upper surface pressures at about 70% chord is predicted. Good correlation is shown for the fuselage bottom centerline pressure distribution. Store surface pressures appear in figure 10. Strong shocks which are predicted towards the aft end of the store do not occur in the data, again possibly due to viscous effects and/or flow separation. These discrepancies also compromise the store axial load distribution correlations, which appear in figure 11. Overall, correlation with data is fair, but not as good as for the subsonic case.

CONCLUDING REMARKS

Correlations indicate that the Transonic Store Carriage Loads Prediction Code provides reliable prediction of store carriage aerodynamics, but that even simple 2-D or axisymmetric modelling of viscous effects and flow separation would improve store carriage loads prediction accuracy. A limited supersonic freestream capability was also demonstrated. Even with the limitations of the transonic small disturbance, embedded grid formulation, the method provides a fundamental understanding of store/airframe interactions not available by other means.

REFERENCES

1. Boppe, C.W., "Transonic Flow Field Analysis for Wing-Fuselage Configurations," NASA CR 3243, May 1980.

2. Boppe, C.W., "Aerodynamic Analysis for Aircraft with Nacelles, Pylons, and Winglets," NASA CR 4066, Apr. 1987.

3. Rosen, B.S., "Computational Transonic Analysis of Canted Winglets," Journal of Aircraft, Vol. 21, No. 11, pp. 873-878, Nov. 1984.

4. Thompson, D.S., "A Mesh Embedding Approach for Prediction of Transonic Wing/Body/Store Flow Fields," paper presented at the Numerical Boundary Condition Procedures Symposium, Moffet Field, CA, 19-20 Oct. 1981.

5. Thompson, D.S., "TAS - A Transonic Aircraft/Store Flow Field Prediction Code," NASA CR 3721, Dec. 1983.

6. Dougherty, F.C., Benek, J.A. and Steger, J.L., "On Applications of Chimera Grid Schemes to Store Separation," NASA TM 88193, Oct. 1985.

7. Lijewski, L.E., "Transonic Flow Solutions on a Blunt, Finned Body of Revolution Using the Euler Equations," AIAA Paper 86-1082, May 1986.

8. Cottrell, C.J. and Lijewski, L.E., "A Study of Finned, Multi-Body Aerodynamic Interference at Transonic Mach Numbers," AIAA Paper 87-2480, Aug. 1987.

9. Rosen, B.S., "Body Flow Field Simulation and Force/Moment Prediction at Transonic Speeds," AIAA Paper 85-0423, Jan. 1985.

10. Rosen, B.S., "External Store Carriage Loads Prediction at Transonic Speeds," AIAA Paper 88-0003, Jan. 1988.

11. Jameson, A., "Iterative Solution of Transonic Flows over Airfoils and Wings, Including Flows at Mach 1," Communications on Pure and Applied Mathematics, Vol. 27, pp. 283-309, 1974.

12. Roache, P.J., "Computational Fluid Dynamics," Hermosa Publishers, Albuquerque, N.M., 1972.

13. Allen, J.H., "Estimation of the Forces and Moments Acting on Inclined Bodies of Revolution of High Fineness Ratio," NACA RM A9I26, 1949.

14. Muse, T.C. and Bratt, R.W., "Summary of High Speed Wind-Tunnel Tests of a Douglas Aircraft Store Shape and a 2000-Pound G.P.-AN-M66 Bomb," Douglas Aircraft Company, Inc. Report E.S. 21150, Jun. 1948.

15. Melnik, R.E., Chow, R.R., Mead, H.R. and Jameson, A., "An Improved Viscid/Inviscid Interaction Procedure for Transonic Flow over Airfoils," NASA CR 3805, Oct. 1985.

16. Stahara, S.S. and Crisalli, A.J., "Data Report for a Test Program to Study Transonic Flow Fields about Wing-Body/Pylon/Store Combinations," AFOSR TR-79-1070, May 1978.

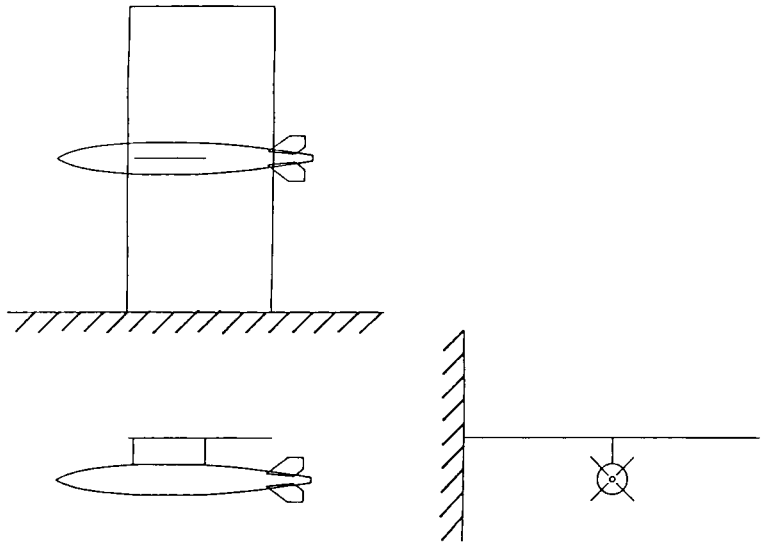

Figure 1. Input geometry verification for Douglas wing/pylon/store.

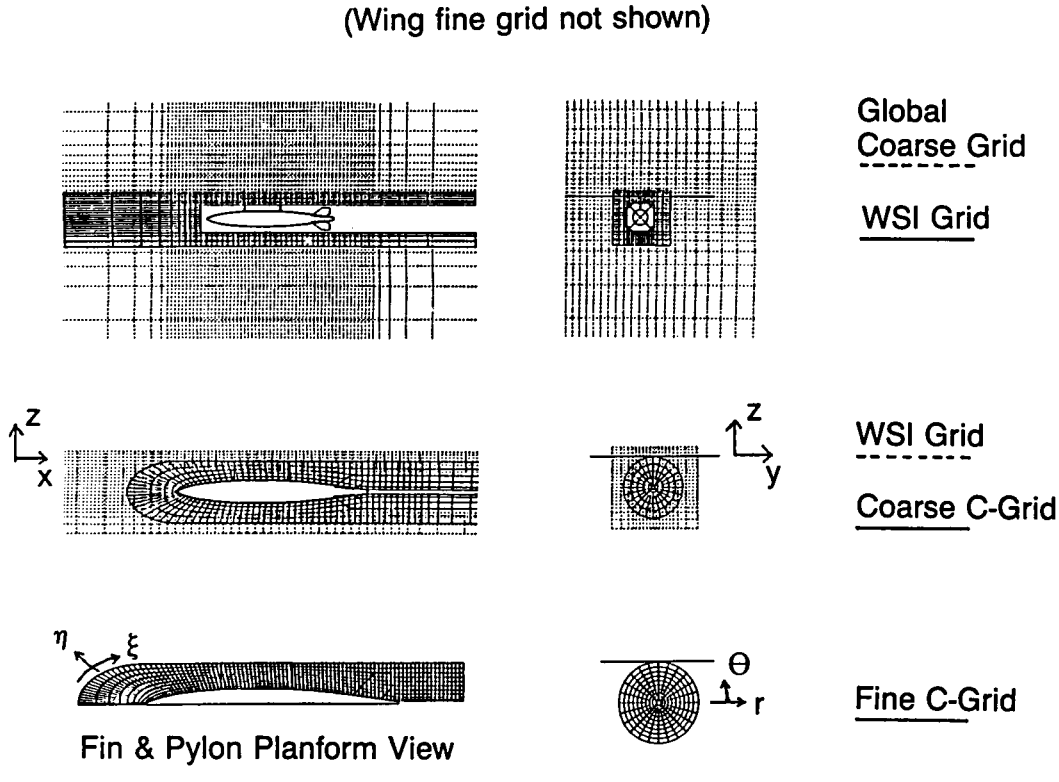

Figure 2. Grid arrangement for Douglas wing/pylon/store.

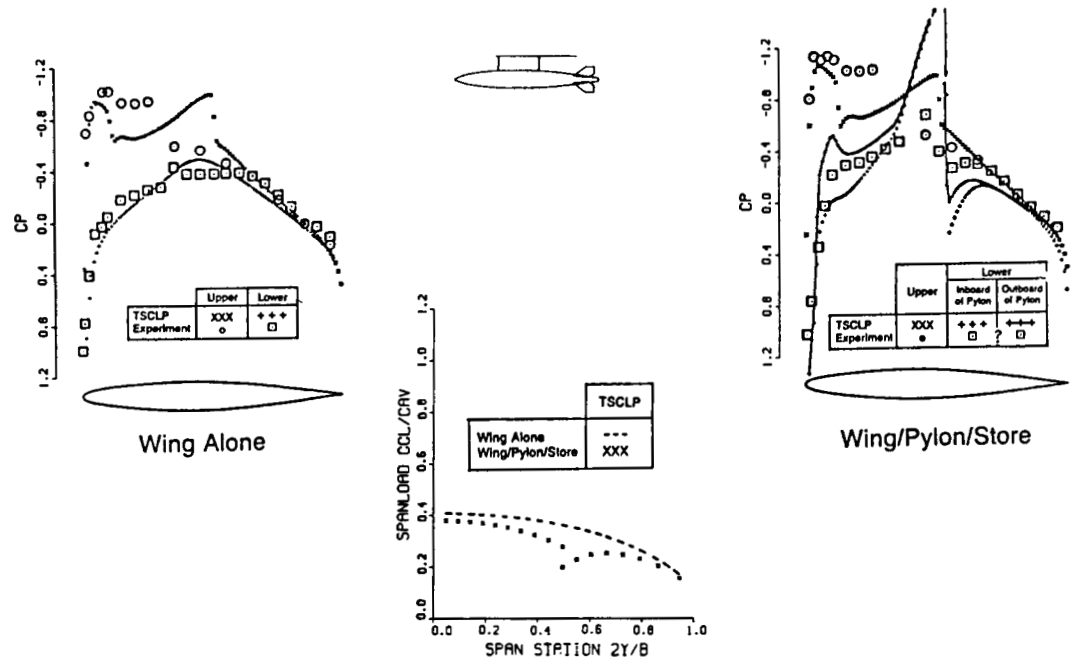

Figure 3. Douglas wing/pylon/store: wing pressure/spanload comparisons at $M_\infty = 0.75$ and $\alpha = 4°$.

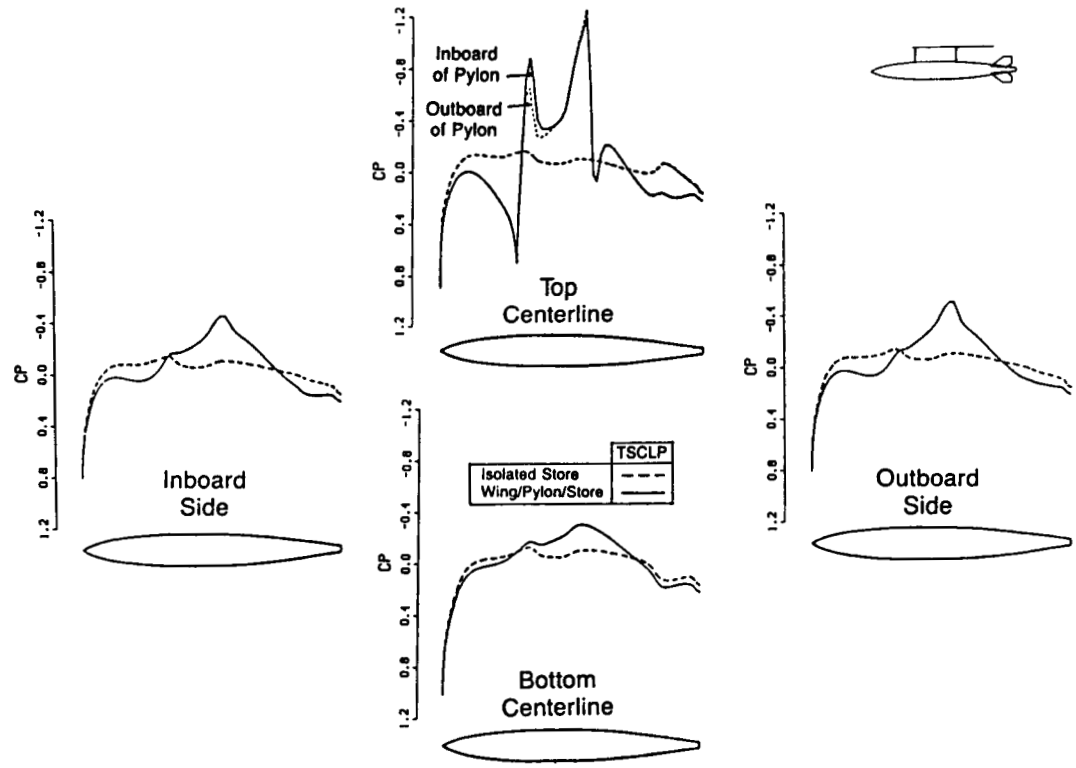

Figure 4. Douglas wing/pylon/store: store body pressure comparisons at $M_\infty = 0.75$ and $\alpha = 4°$.

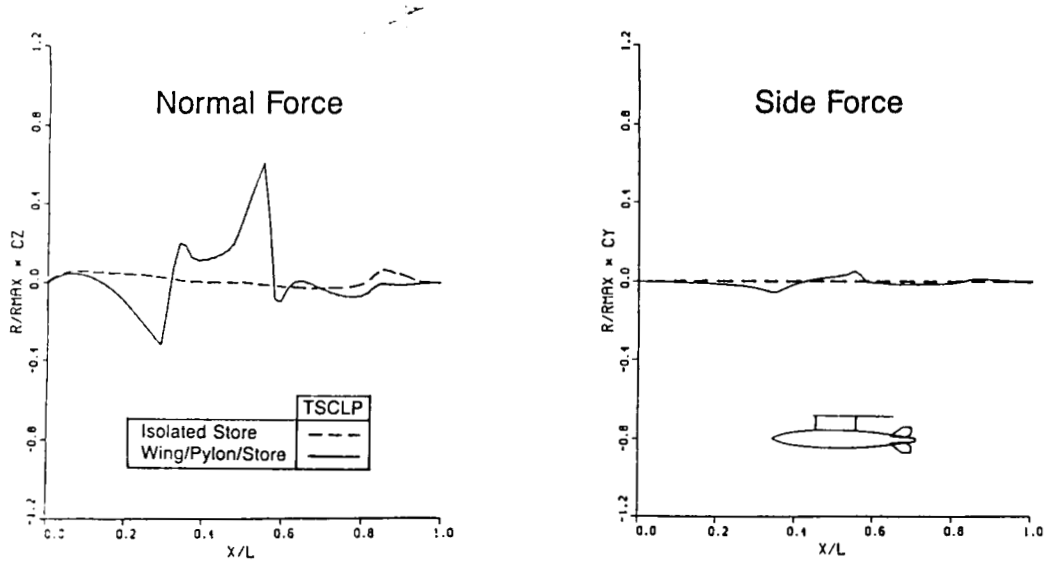

Figure 5. Douglas wing/pylon/store: store body load distribution comparisons at M_∞ = 0.75 and α = 4°.

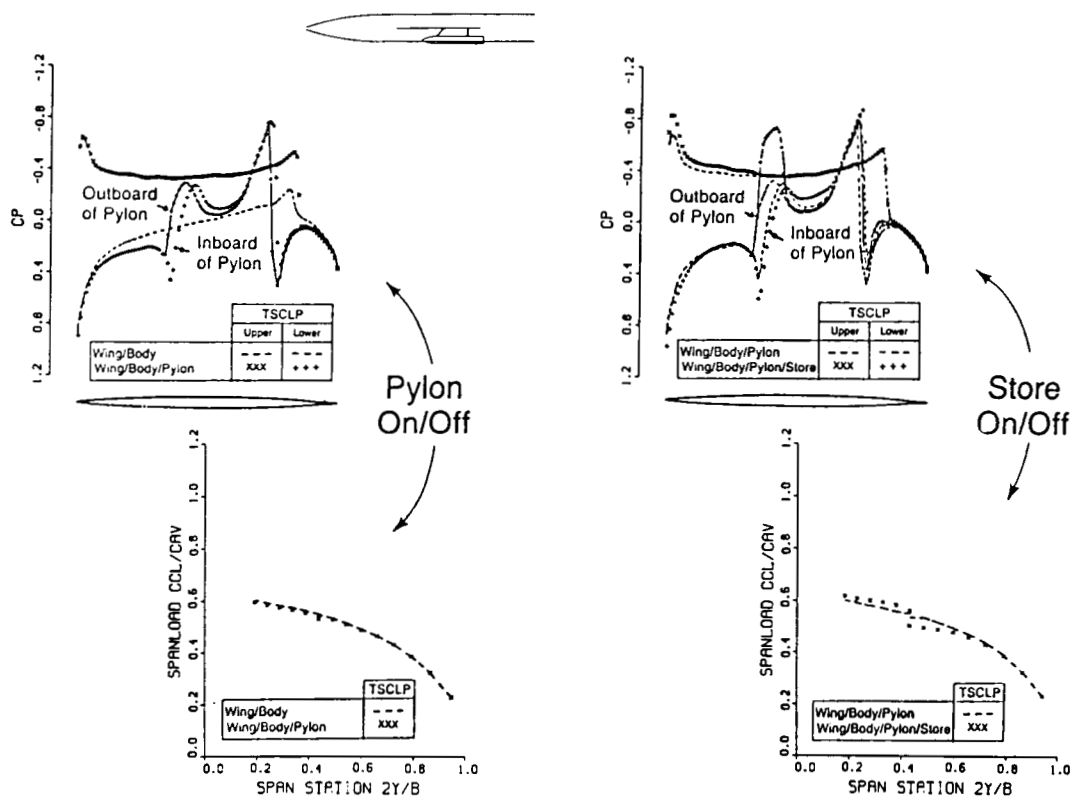

Figure 6. Nielsen wing/fuselage/pylon/store: wing pressure/spanload comparisons at M_∞ = 0.925 and α = 5°.

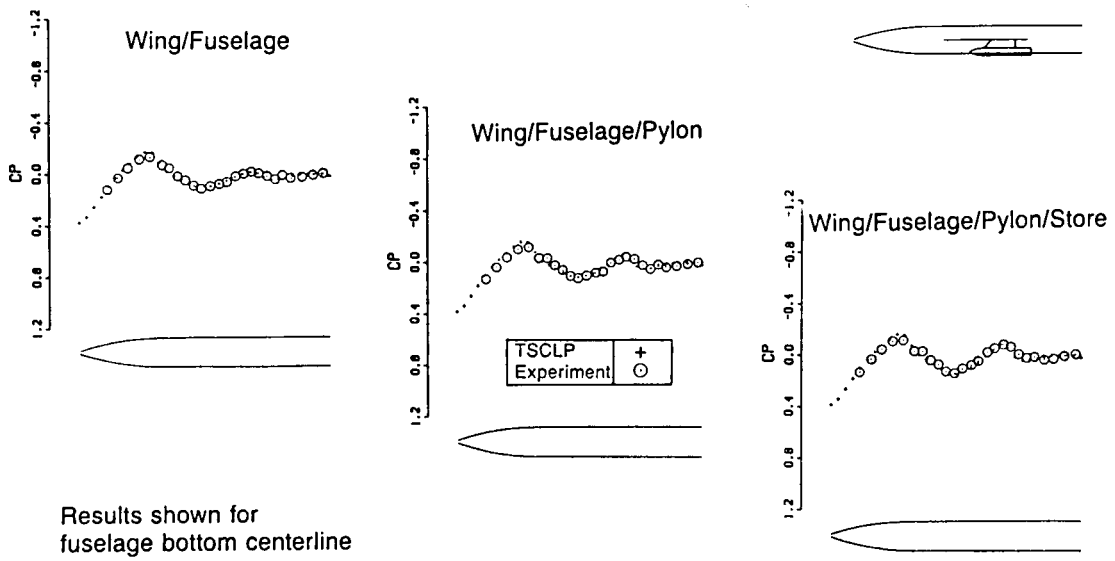

Figure 7. Nielsen wing/fuselage/pylon/store: fuselage pressure comparisons at $M_\infty = 0.925$ and $\alpha = 5°$.

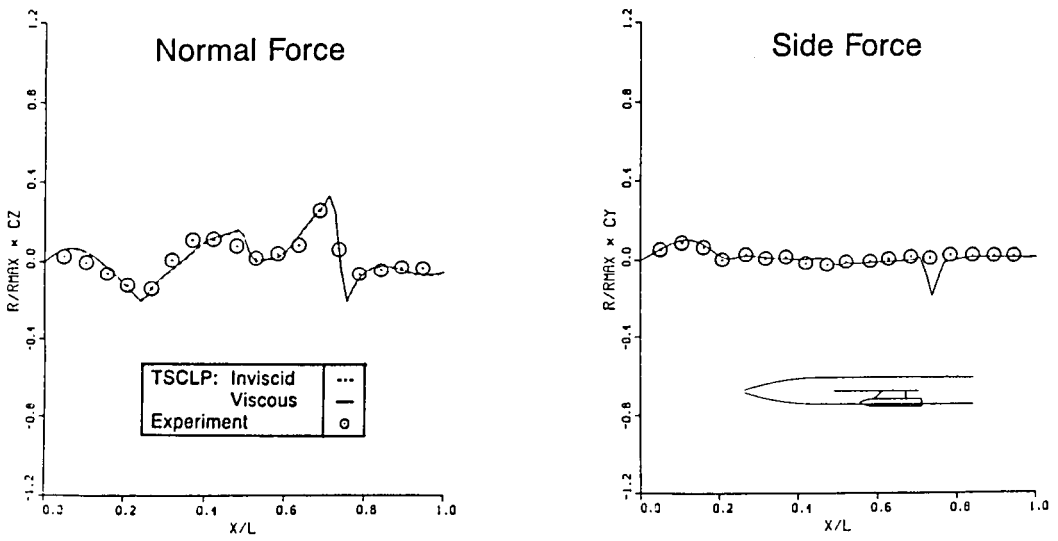

Figure 8. Nielsen wing/fuselage/pylon/store: store load distribution comparisons at $M_\infty = 0.925$ and $\alpha = 5°$.

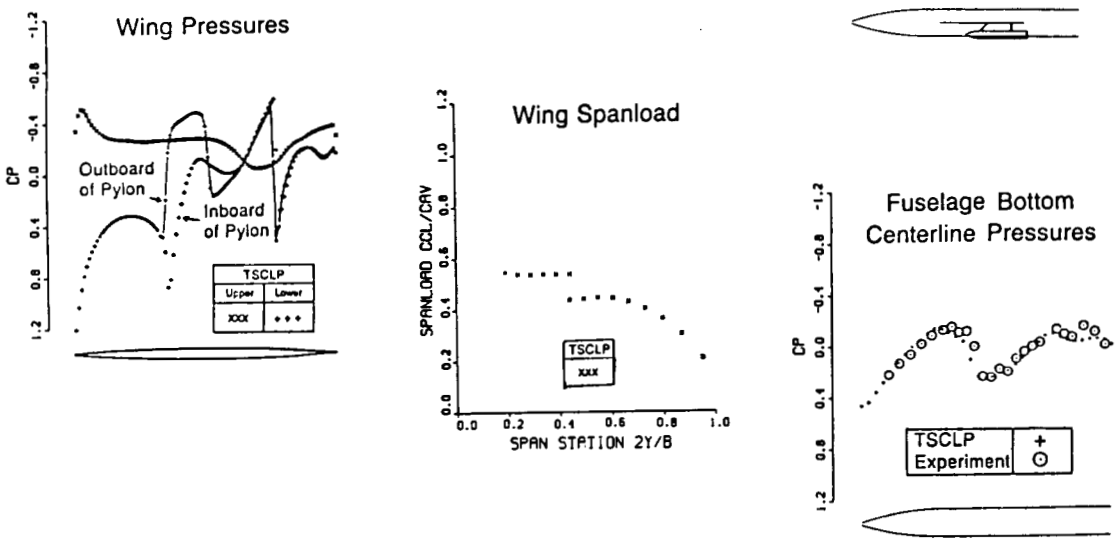

Figure 9. Nielsen wing/fuselage/pylon/store: wing/fuselage pressure/spanload comparisons at M_∞ = 1.1 and α = 5°.

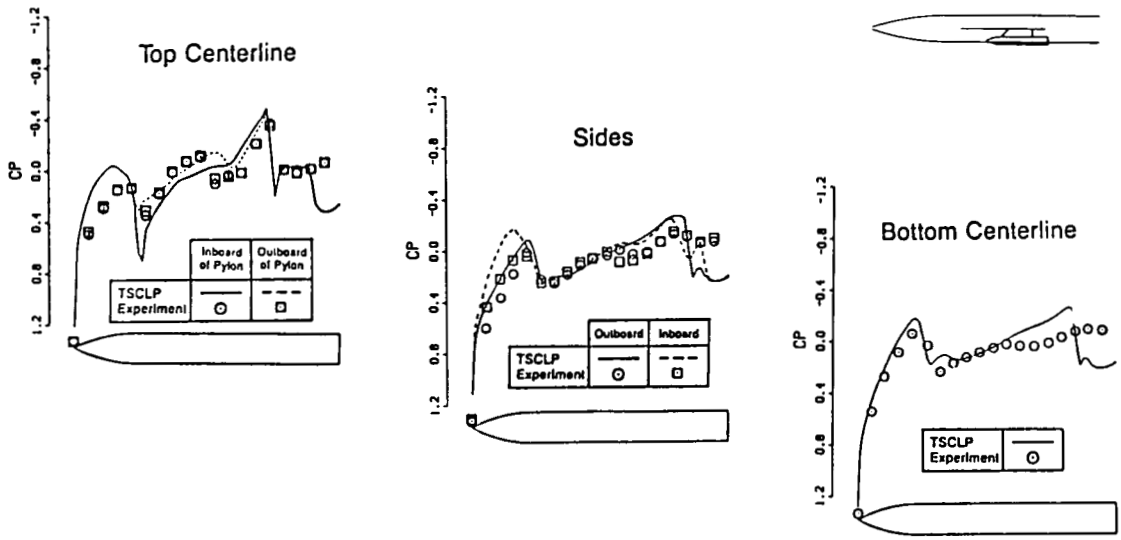

Figure 10. Nielsen wing/fuselage/pylon/store: store pressure comparisons at M_∞ = 1.1 and α = 5°.

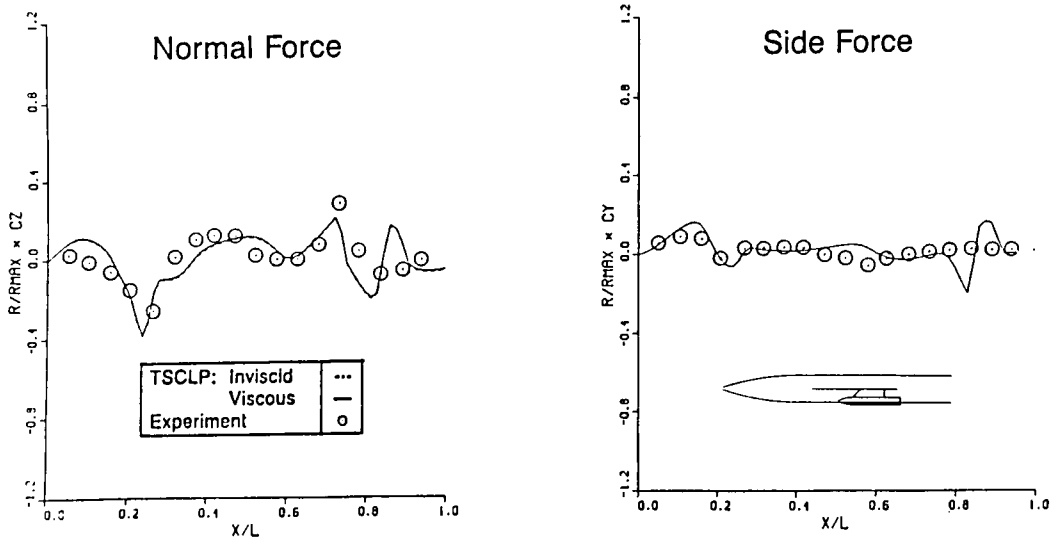

Figure 11. Nielsen wing/fuselage/pylon/store: store load distribution comparisons at $M_\infty = 1.1$ and $\alpha = 5°$.